

# 1 Multi-scenario urban flood risk assessment by integrating future 2 land use change models and hydrodynamic models

3 Qinke Sun<sup>1,2</sup>, Jiayi Fang<sup>1,2</sup>, Xuewei Dang<sup>3</sup>, Kepeng Xu<sup>1,2</sup>, Yongqiang Fang<sup>1,2</sup>, Xia Li<sup>1,2</sup>, Min Liu<sup>1,2</sup>

4 <sup>1</sup>School of Geographic Sciences, East China Normal University, Shanghai 200241, China

5 <sup>2</sup>Key Laboratory of Geographic Information Science (Ministry of Education), East China Normal University, Shanghai  
6 200241, China

7 <sup>3</sup>Faculty of Geomatics, Lanzhou Jiaotong University, Lanzhou 730070, China

8

9 *Correspondence to:* Jiayi Fang (jyfang822@foxmail.com); Min Liu (mliu@geo.ecnu.edu.cn)

10 **Abstract.** Urbanization and climate change are the critical challenges in the 21<sup>st</sup> century. Flooding by extreme weather  
11 events and human activities can lead to catastrophic impacts in fast-urbanizing areas. However, high uncertainty in climate  
12 change and future urban growth limit the ability of cities to adapt to flood risk. This study presents a multi-scenario risk  
13 assessment method that couples the future land use simulation model (FLUS) and floodplain inundation model (LISFLOOD-  
14 FP) to simulate and evaluate the impacts of future urban growth scenarios with flooding under climate change (two  
15 representative concentration pathways (RCPs 2.6 and 8.5)). By taking coastal city of Shanghai as an example, we then  
16 quantify the role of urban planning policies in future urban development to compare urban development under multiple  
17 policy scenarios (Business as usual; Growth as planned; Growth as eco-constraints). Geospatial databases related to  
18 anthropogenic flood protection facilities, land subsidence, and storm surge are developed and used as inputs to the  
19 LISFLOOD-FP model to estimate flood risk under various urbanization and climate change scenarios. The results show that  
20 urban growth under the three scenario models manifests significant differences in expansion trajectories, influenced by key  
21 factors such as infrastructure development and policy constraints. Comparing the urban inundation results for the RCP2.6  
22 and RCP8.5 scenarios, the urban inundation area under the growth as eco-constraints scenario is less than that under the  
23 business as usual scenario, but more than that under the growth as planned scenario. We also find that urbanization tends to  
24 expand more towards flood-prone areas under the restriction of ecological environment protection. The increasing flood risk  
25 information determined by model simulations help to understand the spatial distribution of future flood-prone urban areas  
26 and promote the re-formulation of urban planning in high-risk locations.

## 27 1 Introduction

28 Climate change and urbanization are the global challenges for the 21<sup>st</sup> century ( Ramaswami et al., 2016; Pecl et al., 2017).  
29 Floods have been key threats for many cities around the world driven by global climate change (Hallegatte et al., 2013;  
30 IPCC, 2014; Fang et al., 2020). Currently, more than 600 million people worldwide live in coastal cities that are less than 10

31 m above sea level (United Nations, 2017). The United Nations reports that the global population living in cities is projected  
32 to reach 6.7 billion by 2050 (United Nations, 2018), especially in low elevation coastal areas, the population density is  
33 expected to be twice the current population density (Van Coppenolle and Temmerman, 2019), which means that the  
34 population of coastal cities will become increasingly concentrated in the future and impervious surfaces will become more  
35 numerous (Chen et al., 2020; He et al., 2021). On the other hand, the National Oceanic and Atmospheric Administration  
36 (NOAA) report suggests that global mean sea level will rise around 0.2 m to 2.0 m by 2100 under a continuing global  
37 warming trend (Parris et al., 2012). Additionally, properties and populations in many coastal areas will suffer more severely  
38 in the future if the effects of land subsidence are taken into account (Vousdoukas et al., 2018).

39 However, high uncertainty in flood risk and urban growth leads to a lack of capacity of cities to respond to the flooding  
40 arising from future climate change (Du et al., 2015; Tessler et al., 2015; Fang et al., 2021). Therefore, there is an urgent need  
41 for specialist knowledge and techniques to address the conflict between urbanization and flood risk (Wang et al., 2015; Lai  
42 et al., 2016; Bouwer, 2018; Haynes et al., 2018). Studies on urban flood risk assessment are more likely to simulate flood  
43 risk using different climate change scenarios or integrating different flood sources (Huong and Pathirana, 2013; Muis et al.,  
44 2015; Dullo et al., 2021). For example, Zhou et al. examine the impact of urban flood volumes and associated risks under  
45 RCP2.6 and RCP8.5 scenarios (Zhou et al., 2019). Parodi et al. integrate the compound flood scenarios such as wave height,  
46 storm surge, and extreme sea level due to sea level rise to assess coastal flood risk (Parodi et al., 2020). However, ignoring  
47 the uncertainty of urban growth in urban flood risk assessment reduces the validity of the assessment (Gori et al., 2019), and  
48 hence an increased understanding of possible urban growth scenarios is needed, otherwise there is a lack of understanding of  
49 the consequences of future flooding (Zhao et al., 2017; Kim and Newman, 2020). Although there are some studies have  
50 quantified urban growth and assessed flood risk, such as Chennai (Nithila Devi et al., 2019), Guangzhou (Lin et al., 2020),  
51 Shanghai (Shan et al., 2022), these studies have not considered the development of urban areas under different growth  
52 scenarios and the assessment of flood impacts after the implementation of these scenarios. In addition, the failure to integrate  
53 with broader climate change-related scenarios and possible extreme-case flood risks has led to underinvestment in climate  
54 adaptation actions by governments that do not well address the spatial consequences of future floods (Reckien et al., 2018;  
55 Berke et al., 2019). Thus, there is an urgent need to adopt a more comprehensive approach to assess the complexity of  
56 multiple possible scenarios of urbanization and dynamic flood risk in an integrated manner.

57 This paper uses the coupling of the future land use simulation model (FLUS) and the 2D floodplain inundation model  
58 (LISFLOOD-FP) to explore the possible interaction between different urbanization development scenarios and climate  
59 change scenarios. The FLUS model improves the simulation accuracy of the model by combining artificial neural network  
60 (ANN) and Cellular automata (CA) model to simulate nonlinear land use changes while considering parameters related to  
61 environment, society, climate change, etc. (Liu et al., 2017; Zhai et al., 2020). The LISFLOOD-FP model has become a  
62 mature hydrodynamic model that can predict potential flood events in near real-time and is widely used in engineering  
63 applications (Wing et al., 2019; Sosa et al., 2020). The coastal metropolitan Area of Shanghai in the Yangtze River Delta in  
64 China, one of the fastest urbanizing cities in the world, is used as a case study.

**Deleted:** Although there are some studies that have quantified future growth scenarios for urbanization (Nithila Devi et al., 2019; Lin et al., 2020; Shan et al., 2022), these studies have not considered the impact of existing planned policies that are designed to mitigate the impact of new development.

**Deleted:** are

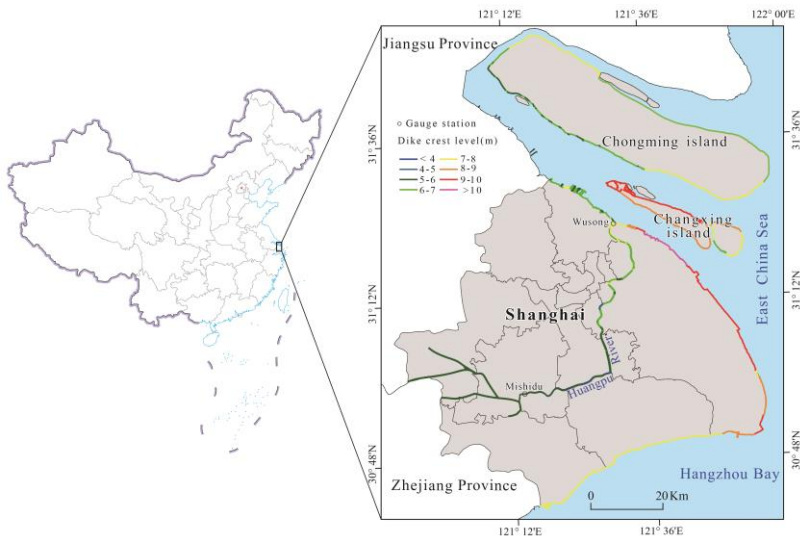
71 The paper asks, how different urban growth scenarios combined with climate change scenario analysis may help to inform  
72 preparedness for flood risks from climate change in urban flood risk assessments? To answer this question, we first assume  
73 some future simulation scenario by considering the factors that influence urban growth and lead to flood risk. Secondly, we  
74 coupled urban growth and flood risk scenarios and compared them using climate change scenarios from two representative  
75 concentrated pathways (RCP 2.6 and 8.5) proposed by the Intergovernmental Panel on Climate Change (IPCC). Finally, we  
76 assessed the risk of flooding in different urban development scenarios. The research illustrates the importance of assessing  
77 the performance of different future urban development scenarios in response to climate change, and the simulation study of  
78 urban risks will prove to decision-makers that incorporating disaster prevention measures into urban development plans will  
79 help to reduce disaster losses and improve the ability of urban systems to respond to floods.

## 80 **2 Study area and datasets**

### 81 **2.1 Study area**

82 As the alluvial plain of the Yangtze River Delta, Shanghai is located on the coast of the East China Sea between 30°40′–  
83 31°53′N and 120°52′–122°12′E, which borders the provinces of Jiangsu and Zhejiang to the West (Fig. 1). It's a typical  
84 middle latitude transition belt, marine land transitional zone and also a typical estuarine and coastal city with a fragile  
85 ecological environment. The land area of Shanghai is about 6340.50 km<sup>2</sup>, accounting for 0.06 % of the total area of China,  
86 and has 213 km of coastlines. The Shanghai metropolitan area has undergone rapid urban expansion in the past decades and  
87 has become one of the largest urban areas in the world in both size and population (Sun et al., 2020). However, Shanghai's  
88 topography is low, with an average elevation of 4 m above sea level, and there is no natural barrier against storm surges. In  
89 1905, one of the deadliest storm surges occurred in Shanghai, killing more than 29,000 people. Two years later, Typhoon  
90 Winnie made landfall in Shanghai, flooded more than 5,000 households (Du et al., 2020). Additionally, due to land  
91 subsidence and the increasing frequency and intensity of storm surges, Shanghai will become one of the most sensitive  
92 regions due to global climate change.

**Deleted:** The rest of paper is organized as follows: section 2 describes the characteristics of the study area and presents the data used in this paper; followed by a description of the methodology for integrating future land use change models and hydrodynamic models in Section 3. The results and discussion in Section 4 and Section 5. We divided the discussion section into two parts, on the one hand discussing the sources of uncertainty in the study, and the other part discussing adaptation policies for urban flood risk in the context of climate change. The conclusion of the study is described in Section 6.



102  
 103 **Figure 1: Location map of the study area. The main inland rivers in Shanghai flow into the East China Sea through the Huangpu**  
 104 **River. The line with coloured vectors in the figure indicates the different dike crest level in Shanghai.**

105 **2.2 Data**

106 The research used three main categories of data, including basic data, scenarios constraints data and flood simulation data  
 107 (Table 1). The basic data include land use, topography, traffic network, traffic site, socio-economic data. The land use data  
 108 with a resolution of 100 m×100 m from the Resource and Environmental Science and Data Center of the Chinese Academy  
 109 of Sciences is currently the most accurate land use remote sensing monitoring data product in China (Liu et al., 2014). The  
 110 data for 2005 and 2010 were derived from Landsat-TM/ETM remote sensing image data respectively, and the data for 2015  
 111 were interpreted using Landsat 8 remote sensing image. After the data were corrected and visually interpreted, the  
 112 comprehensive evaluation accuracy of the interpretation accuracy of the first-class types of cultivated land, woodland,  
 113 grassland, water area, urban land, and unused land reached more than 94.30 %, and the discrimination accuracy rate on the  
 114 map patches reached 98.70 % (Xu et al., 2017). Within the allowable error range, it can be used as the basic data for  
 115 analyzing land use changes.

116 Topography factors (DEM, slope), traffic network factors (distance to railway, highway, subway, and main roads), traffic  
 117 site factors (distance to the city center, train station, and airports) and socio-economic factors (population, GDP), etc. as well  
 118 as planning constraints, were determined to be spatial influence factors of the flood risk assessment of the Shanghai area.

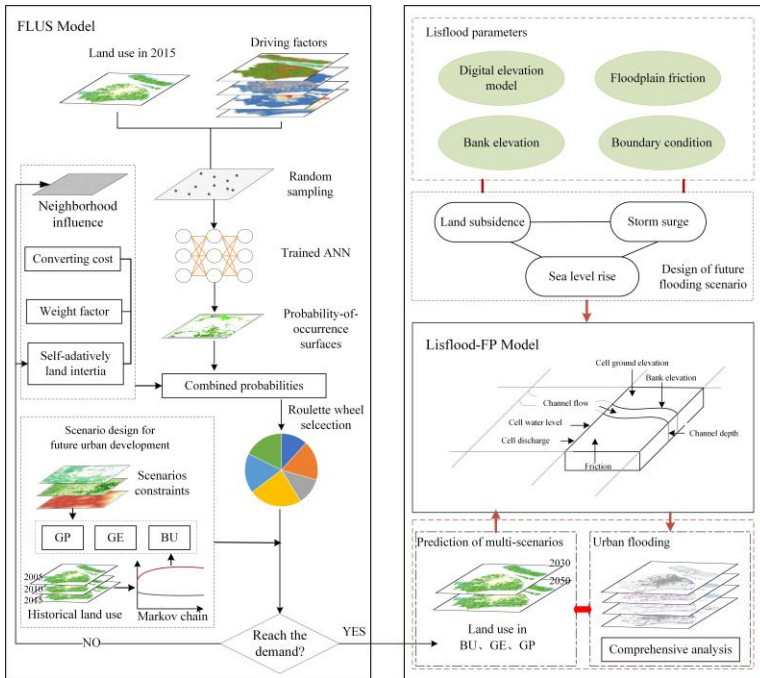
119 The Advanced Spaceborne Thermal Emission and Reflection Radiometer (ASTER) digital elevation model (DEM), which  
 120 has 30-meter resolution, served as the basis data for terrain heights and slopes. ASTER-DEM has been shown to be the most  
 121 stable data performer among six types of open access DEM products (SRTM, ASTER-DEM, AW3D, MERIT, NASADEM  
 122 and CoastalDEM) for flood inundation simulations with different return periods (Xu et al., 2021). Traffic network and site  
 123 were collected from open-source data retrieved from OpenStreetMap (OSM) and POI data were extracted from Tencent  
 124 Map. Euclidean distance was calculated for all vector data. The data of population and gross domestic product (GDP), were  
 125 provided by the Resource and Environmental Science and Data Center of the Chinese Academy of Sciences (Xu, 2017a,  
 126 2017b), and their time span was consistent with the land use data. According to the simulation forecast demand, all materials  
 127 were converted into  $100 \times 100$  m grid by resampling. The spatial limiting factors were the basic ecological control line,  
 128 permanent basic cropland and cultural protection control line as outlined in the 2017–2035 Shanghai City Master Plan. All  
 129 the impact factor data were normalized, and the range of the value is between 0 and 1 to subsequent data mining.  
 130 The storm surge data comes from the Global Tide and Surge Reanalysis (GTSR) dataset, which has been validated to have  
 131 good accuracy (Muis et al., 2016). In addition, man-made flood defenses have been considered to reasonably evaluate the  
 132 inundation impact of the flooding. The coastal flood protection data was obtained from the historical archival of the  
 133 Shanghai Water Authority for Shanghai (Yin et al., 2020). All data sources are listed in the table below.  
 134 **Table 1. Data required and sources. The list details the resolution and sources of the data in the study.**

Category	Data Type	Resolution	Source
Basic data	Land use	100 m $\times$ 100m	Resource and Environmental Science and Data Center ( <a href="http://www.resdc.cn">http://www.resdc.cn</a> )
	Topography	Vector line	ASTER GDEM ( <a href="https://earthexplorer.usgs.gov/">https://earthexplorer.usgs.gov/</a> )
	Traffic network	Vector line	OpenStreetMap ( <a href="https://www.openstreetmap.org">https://www.openstreetmap.org</a> )
	Traffic site	Vector point	Tencent Map ( <a href="https://map.qq.com/">https://map.qq.com/</a> )
	Social economy	1 km $\times$ 1 km	Resource and Environmental Science and Data Center
Scenarios constraints	Ecological control line	Vector line	《2017-2035 Shanghai City Master Plan》
	Permanent basic cropland control line	Vector line	
	Cultural protection control line	Vector line	
Flood data	Floodwalls	Vector line	Shanghai Water Authority ( <a href="http://swj.sh.gov.cn/">http://swj.sh.gov.cn/</a> )
	Storm surge	Vector line	GTSR

Deleted: in

136 **3 Methodology**

137 The presented approach for relative sea level rise scenario flood risk assessment is the integration of the FLUS model,  
 138 LISFLOOD-FP model, and Markov chain model. In the framework, the FLUS model and Markov chain model are designed  
 139 to stimulate complex land-use change processes in three different scenarios through 2030 to 2050, which include Business as  
 140 usual (BU), Growth as planned (GP), Growth as eco-constraints (GE) scenarios. A Markov chain model is used to predict  
 141 land-use demand in 2030 and 2050, combining planning policy factors, which is one of the crucial data inputs in the FLUS  
 142 model. Next, the LISFLOOD-FP two-dimensional flood model is used to explore the potential flooding areas under the RCP  
 143 2.6 and 8.5 scenarios in 2030 and 2050, to avoid the overestimation of the submerged range based on the GIS-based  
 144 elevation area method. This model also considers the compound influence of sea-level rise, storm surge, and land  
 145 subsidence. Finally, via ArcGIS spatial comprehensive analysis, the flooding of different land types is calculated employing  
 146 different flooding scenarios. The overall flow chart of research is illustrated in Fig. 2.



147  
 148 **Figure 2: The overall flow chart of research.**

149 **3.1 Markov chain model**

150 Markov chain model refers to the random transition process of state from one state to another, and its future state is only  
151 related to the state at previous moment. In the study of land use change, the type of land use at a certain moment is only  
152 related to the type of land use at the previous moment. Therefore, land-use change is a typical Markov process and has  
153 widely used in the prediction of land-use changes (Zhou et al., 2020). We predicted future land use by Eq. (1):

154 
$$S_{(t+1)} = P_{i,j} \times S_t \quad (1)$$

155 where  $S_t$  and  $S_{t+1}$  represent the land use at times  $t$  and  $t+1$ , and  $P_{i,j}$  is a state transition matrix that land-use type  $i$  is  
156 converted to land-use type  $j$ . This model has a good predictive effect on the process state (Gounaridis et al., 2019).  
157 Therefore, we use the Markov chain to calculate the probability of the conversion of various land types, and then predict the  
158 number of future land changes.

159 **3.2 The FLUS land use simulation model**

160 The FLUS model is an upgraded version of a cellular automata model (Liu et al., 2017) which can solve the complex land  
161 use simulation problems by self-adaptive inertia and competition mechanism. The FLUS shows the highest current  
162 performances than other simulation models such as CLEU-S, SLEUTH, and LTM and has been applied to land use change  
163 simulation research at different scales and for different purposes (Liang et al., 2018; Lin et al., 2020).

164 As the most important scheme to manage the space of the urban area, an urban land use plan can reflect the general  
165 arrangement of land use in the future (Xu and Yang, 2019). In this research, three categories of urban growth scenarios are  
166 simulated through the FLUS model. The similarity of the three scenarios is that they use factors that affect urban  
167 development and changes, such as population, GDP, traffic, and slope, as the main spatial driving factors. The difference are  
168 as follows:

169 (i) Business as usual (BU): BU is natural growth without development laws and regulations. Its development is based on the  
170 premise of the current urban development patterns. Therefore, the land demand predicted by Markov is used as the constraint  
171 condition for the iteration of CA model in the subsequent application of the scenario.

172 (ii) Growth as planned (GP): Under the GP scenario, the urban growth projection that closely link to the master plan for  
173 Shanghai in terms of quantity, reflecting how the city government prefer to develop. The master plan requires that the total  
174 area of planned urban construction land does not exceed 3,200 km<sup>2</sup> in 2035. We choose an urban area of 2768 km<sup>2</sup> in 2030  
175 and 3200 km<sup>2</sup> in 2050 as the constraints under the GP scenario. The reason is that the Markov chain model projections result  
176 in an urban area is 2768 km<sup>2</sup> in 2030 and 3270 km<sup>2</sup> in 2050, and the total urban construction land area in 2035 of the  
177 Shanghai Master Plan does not exceed 3200 km<sup>2</sup>.

178 (iii) Growth as eco-constraints (GE): The GE scenario is an eco-environmental protection scenario which development is  
179 limited by the ecological environment protection. Combined with Shanghai's ecological and environmental protection

180 requirements and the distribution of permanent basic farmland, sensitive areas restricted for development are identified at the  
181 scenario, and we also establish a cultural protection control line for strengthening historical and cultural protection. In  
182 addition, the number of areas of future urban growth in the GE scenario also combines the requirements given in the urban  
183 master plan to enhance the reality of the scenario.

184 Therefore, the FLUS model is used to simulate future urban growth combining various scenarios. First, the driving factors  
185 and land-use data are trained by an ANN model to obtain a probability-of-occurrence map, and then incorporate with the  
186 self-adaptive land inertial, conversion cost, and neighborhood competition among the different land use types to estimate the  
187 combined probability for each grid. Next, combining the number of various types of land predicted by the Markov Chain  
188 model and considering the constraints of each scenario to predicted urban growth in 2030 and 2050. To better validate the  
189 model before predicting future change, we compared the output with the actual land use 2015. Note that the number of  
190 iterations in each scenario is set to 5000, which is much higher than the default value to show higher prediction accuracy.

### 191 **3.3 The LISFLOOD-FP flood inundation model**

192 LISFLOOD-FP is a 2D hydraulic model based on a raster grid (Bates et al., 2010), which can efficiently simulate the  
193 dynamic propagation of flood waves over fluvial and estuarine floodplains and show real-time changes in water depth of  
194 complex terrain. LISFLOOD-FP model solves the Saint-Venant equations at very low computational cost by omitting only  
195 the convective acceleration term over a structured grid using a highly efficient explicit finite difference scheme to produce a  
196 two-dimensional simulation of floodplain hydrodynamics (O'Loughlin et al., 2020). The model has been widely used in the  
197 applications of small-scale and large-scale urban waterlogging and flooding (Hoch et al., 2019; Rajib et al., 2020; Zhao et  
198 al., 2020).

199 In the present study, the LISFLOOD-FP model is used to simulate storm surge floods along the coast of Shanghai and floods  
200 along the Huangpu River. The effectiveness of the model in the study area has been verified by another article of our group  
201 members and shows good simulation results(Xu et al., 2021). In the boundary control of model, hydrological stations and  
202 global storm surge data are respectively employed as the input of the scenario design. However, Shanghai Geological  
203 Environmental Bulletin and land subsidence control plan show that land subsidence has a significant contribution to the  
204 flood hazards in Shanghai (Xian et al., 2018). Land subsidence in Shanghai is mainly caused by tectonic subsidence and  
205 compaction of sediments due to geological structure conditions and human activities. With reference to the long-term  
206 tectonic subsidence monitoring data of the very long baseline interferometer (VLBI) in the Sheshan bedrock and the land  
207 subsidence analysis rules of Yin et al. (Yin et al., 2013). therefore, the total land subsidence is predicted to be 0.12 m and  
208 0.24 m by 2030 and 2050, respectively. However, due to the uncertainty of future anthropogenic activities and spatial  
209 distribution, there could be large variations in the projection. This study also combines the storyline of future scenarios of the  
210 IPCC, namely the Representative Concentration Pathway (RCP) scenarios, and selects conservative (RCP2.6) and largest  
211 magnitude (RCP8.5) climate-change scenarios, with values from Kopp et al (Kopp et al., 2017). For the simulation of the  
212 Huangpu River flood, we conducted experiments for a 50-year return period under the RCP2.6 scenario and a 100-year

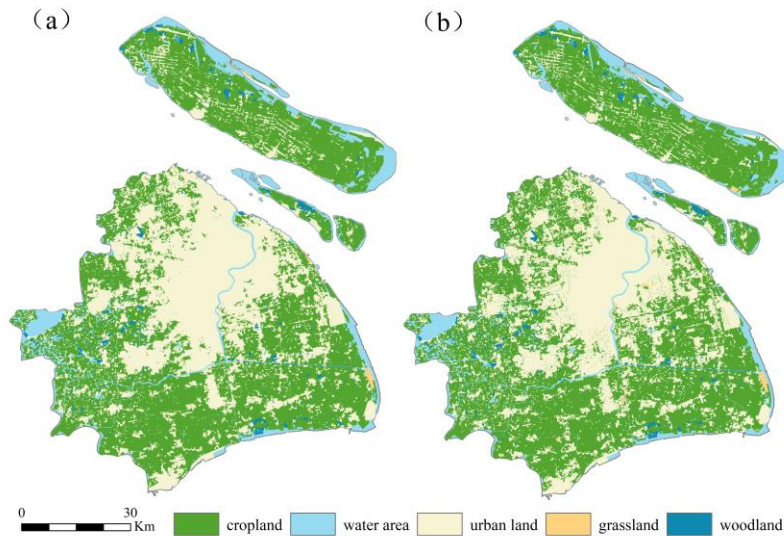


213 return period under the RCP8.5 scenario respectively during 2030 to 2050. For the 2030 and 2050, both Huangpu River and  
214 the coastal floods are following the RCP2.6 and RCP8.5 scenarios. Finally, we combine land subsidence and the RCP data to  
215 control the flood inundation simulation.

## 216 4 Results

### 217 4.1 Model validity

218 Model verification is the prerequisite for model operation, and the operation can only be carried out after confirming the  
219 model to be valid. The applicability of the proposed model was tested by simulating land use/cover changes (LUCC) in 2015  
220 at Shanghai. The spatial simulation result shows that the simulated result and the actual land use have a high consistency  
221 (Fig. 3). We compared the actual land use and the simulated result pixel by pixel in our study and found the overall accuracy  
222 (OA) was 93.20 %, the kappa coefficient (kappa) was 0.89. The discrepancy of the actual land use and simulated result is  
223 likely due to the neighborhood interaction in the CA model, in which grid cells in more urbanized neighborhoods have a  
224 higher probability to convert to urban, whereas the grid cells are less likely to change to urban in less urbanized  
225 neighborhoods. Overall, the measured model accuracy outputs showed an acceptable or good level of prediction, therefore  
226 the model is suitable for predicting changes in land use of the Shanghai area.



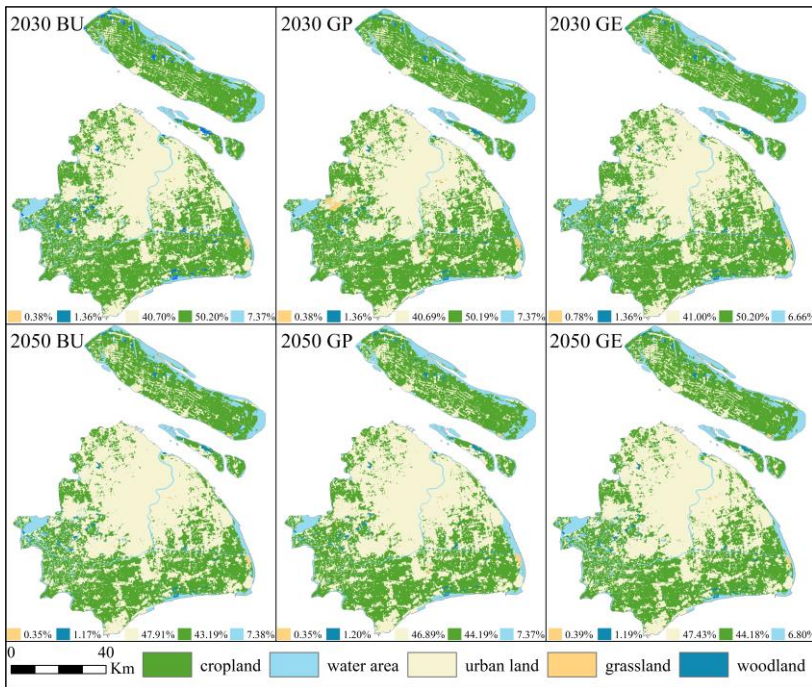
227

228 **Figure 3: Comparing the simulation results of Shanghai urban expansion with the actual situation, (a) simulation result in 2015;**  
229 **(b) actual land use in 2015.**

#### 230 **4.2 Future land use changes**

231 Based on the conditions under three different development scenarios, we predicted the development of future urban land use  
232 change in 2030 and 2050. The prediction result shows different development patterns for each scenario (Fig. 4). Future urban  
233 growth under the BU scenario is primarily located in northwestern with some development in the central regions, and under  
234 the GP scenario the urban growth involves evenly distributed development. Urban growth in the GE scenario, however,  
235 Chongming Island regions have seen more urban growth, and the downtown area is not fully occupied by urban expansion  
236 due to restrictions.

237 Due to the impact of infrastructure construction, distance to the city center, and policy restrictions, Shanghai's overall urban  
238 expansion model shows a center-peripheral expansion. The built-up land areas in 2030 and 2050 are respectively projected to  
239 increase by about 6 % and 13 % as compared to 2015, the most significant reduction is found for cultivated land and  
240 woodland. Specifically, the built-up land areas in 2030 are respectively projected to increase by 427.32 km<sup>2</sup>, 428.27 km<sup>2</sup> and  
241 429.12 km<sup>2</sup> at BU, GP and GE scenarios, the built-up land areas in 2050 are respectively projected to increase by 926.38  
242 km<sup>2</sup>, 857.63 km<sup>2</sup> and 751.47 km<sup>2</sup> at BU, GP and GE scenarios. The most significant reduction is found for cropland, which is  
243 predicting in 2050 to decrease by 876.97 km<sup>2</sup>, 857.63 km<sup>2</sup> and 723.59 km<sup>2</sup> as compared to 2015 in BU, GP and GE  
244 scenarios. The southwestern region is not suitable for large-scale urban development, since large amounts of farmland in the  
245 region are listed as ecological protection areas, so the slow growth of these areas is not expected. The simulation maps show,  
246 as expected, land use changes under different planning scenarios, especially the urban sprawl trend at the GE scenario,  
247 creating new development areas in suburbs. To sum up, the urban expansion trajectory under BU, GP and GE shows  
248 significant differences, and these changes mainly at the expense of the cropland.



249  
 250 **Figure 4: Simulation results of different scenarios in 2030 (top) and 2050 (bottom). Each image shows the spatial distribution and**  
 251 **the proportion of area of different land use types in the simulated scenario.**

#### 252 4.3 Changing flood hazard in the future

253 The LISFLOOD-FP model is used to simulate the flood evolution process under RCP2.6 and RCP8.5 scenarios (the  
 254 inundation results are plotted in Supplementary Figure 1), and then the submerged depth and area under different scenarios  
 255 are statistically analyzed to explore the future flood risk under different RCP scenarios. First, the maximum water depth risk  
 256 of the submerged area is counted, and the submerged area is divided into four depth levels: the submerged water depth is less  
 257 than 0.5 m as shallow water area, water depth is 0.5-1 m as medium water area, the water depth is 1-2 m as deep water area,  
 258 and submerged water depth is above 2 m as the extremely deep area. The area and proportion of each water depth level are  
 259 calculated.

260 By comparing the scenarios in RCP2.6 and RCP8.5, it is evident that the submerged area is increasing with time (Table 2).  
 261 The total flooded area increased by 162.43 km<sup>2</sup> and 189.44 km<sup>2</sup> under RCP2.6 and RCP8.5 scenarios from 2030 to 2050,

262 respectively. Additionally, the depth of submergence and the extent of submergence will gradually increase as the floodwater  
 263 spreads. Taking the area with submergence depth above 2 m as an example, under RCP2.6 scenario the area with  
 264 submergence is 353.69 km<sup>2</sup> and 401.57 km<sup>2</sup> respectively in 2030 and 2050, and under RCP8.5 scenario the area with  
 265 submergence is 356.28 km<sup>2</sup> and 418.36 km<sup>2</sup> respectively in 2030 and 2050. It shows that Shanghai will still face great flood  
 266 risk under these two scenarios.

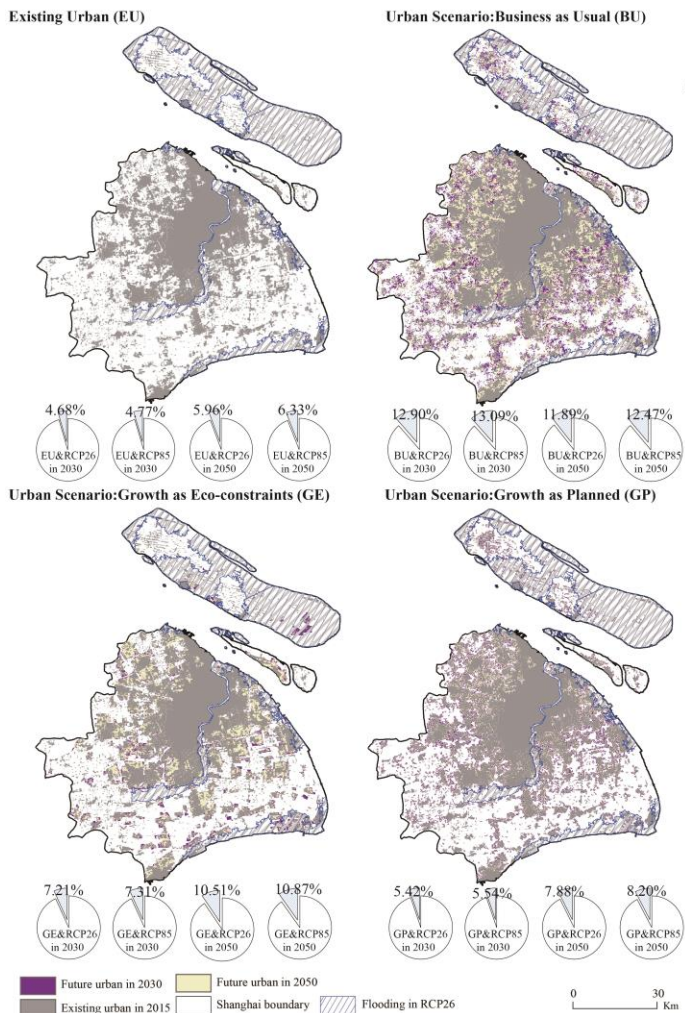
267 **Table 2. Statistics of flood depth.**

Category	<0.5 m		0.5-1 m		1-2 m		>2 m		Total /km <sup>2</sup>
	Area/ km <sup>2</sup>	Ratio/ %	Area/ km <sup>2</sup>	Ratio/ %	Area/ km <sup>2</sup>	Ratio/ %	Area/ km <sup>2</sup>	Ratio/ %	
2030 RCP2.6	138.61	14.54	164.07	17.21	296.98	31.15	353.69	37.10	953.35
2030 RCP8.5	137.13	14.23	169.76	17.61	300.82	31.21	356.28	36.96	963.99
2050 RCP2.6	125.04	11.21	229.81	20.60	359.36	32.21	401.57	35.99	1115.78
2050 RCP8.5	141.72	12.29	219.58	19.04	373.77	32.41	418.36	36.27	1153.43

Deleted: water

#### 268 4.4 Future changes in urban flood risk

269 The flood risk of the urban area is calculated by overlapping existing urban and projected future urban scenarios with future  
 270 flood risk zones. First, in the existing urban exposure to future flood risk scenarios (the upper left in Fig. 5), more urban  
 271 areas will be vulnerable to flood risk in the context of global climate change. The four pie charts for the EU scenarios  
 272 represent the proportion of the existing urban area affected by the future flood risk scenario. Under the RCP 2.6 scenario,  
 273 4.68 % and 5.96 % of the total existing urban areas in 2030 and 2050 would be susceptible to flood risk, respectively. In the  
 274 2030 and 2050 of the RCP8.5 scenarios the area of existing urban land which would be vulnerable to future flood risks are  
 275 110.27 km<sup>2</sup> and 146.23 km<sup>2</sup>, respectively. Many urban areas will be flooded under sea level rise caused by climate change  
 276 even when protected by levees, and more than 5 % of urban areas in Shanghai are still in the floodplain (Fig. 5).



278  
 279 **Figure 5: Flood exposure of existing urban and future urban growth scenarios. The four pie charts for the BU, GE, and GP**  
 280 **scenarios represent the proportion of new grown urban area exposed to flooding under the 2030 RCP2.6, 2030 RCP8.5, 2050**  
 281 **RCP2.6, and 2050 RCP8.5 scenarios, respectively. The four pie charts for the EU scenarios represent the proportion of the existing**  
 282 **urban area affected by the future flood risk scenario.**

283 Future urban development would occur in the flood zone, with a rapid expansion of the urban area. Fig. 5 also shows the  
 284 comprehensive analysis results of the three urban growth scenarios under different climate change scenarios. Under the  
 285 RCP2.6 scenario, new growth in urban land area affected by flooding in 2030 are respectively 55.11 km<sup>2</sup>, 23.22 km<sup>2</sup>, and  
 286 30.92 km<sup>2</sup> at BU, GP and GE scenarios. Under the RCP8.5 scenario, future more urban growth areas would be affected by  
 287 the flooding, which will reach 115.53 km<sup>2</sup>, 70.36 km<sup>2</sup>, and 81.71 km<sup>2</sup> at BU, GP and GE scenarios in 2050, respectively. In  
 288 general, the higher the sea level rises, the greater the risk of flooding in future urban areas. Small changes in sea level rise  
 289 will affect a large amount of land, since the average altitude of Shanghai is only around 4 m.

290 **Table 3. Inundation of each land use type under different scenarios. The inundated areas of different land use types, including**  
 291 **cropland, woodland, grassland and urban land, were calculated for each scenario, where <sup>a</sup> indicates new grown areas of the urban**  
 292 **class affected by flooding.**

Time	Category	Urban scenario	Inundated areas (km <sup>2</sup> )			
			Cropland	Woodland	Grassland	Urban land <sup>a</sup>
2030	RCP2.6	BU	595.05	10.05	5.60	55.11
		GE	618.95	12.12	5.84	30.92
		GP	597.71	12.40	5.91	23.22
	RCP8.5	BU	602.38	10.23	5.67	55.92
		GE	625.97	12.29	5.91	31.23
		GP	604.32	12.59	5.98	23.72
2050	RCP2.6	BU	662.64	13.56	5.25	110.19
		GE	677.59	16.74	5.95	78.95
		GP	651.24	15.66	5.46	67.55
	RCP8.5	BU	683.56	15.06	5.70	115.53
		GE	698.98	18.05	6.40	81.71
		GP	672.30	16.85	5.91	70.36

293  
 294 The research found that the cultivated land is the most affected land type by flooding relative to urban areas, woodland and  
 295 grassland (Table 3). Under the GE scenario, the flooded area of cultivated land is 618.95 km<sup>2</sup> and 625.97 km<sup>2</sup> at the RCP2.6  
 296 and RCP8.5 in 2030, and 677.59 km<sup>2</sup> and 698.98 km<sup>2</sup> at the RCP2.6 and RCP8.5 in 2050. Further, the exposure of various  
 297 types of land is increasing with time, but urban land and cropland will be the most impacted land types in the future.  
 298 Comparing the three scenarios we can find that the urban development area under the planning scenario is less affected by

299 flooding, as compared to the business-as-usual development scenario. Comparing the inundation of the two planning  
300 scenarios (GE and GP), it also reflects the decision-makers' trade-off between economic development and ecological  
301 protection. The inundation area of the urban land under the GP scenario is less than that of the GE, which means that under  
302 the planning constraint of protecting ecological and cultural areas, urban built-up areas will develop on low-protection areas,  
303 which are more vulnerable to flooding. In conclusion, from reducing the risk of future flooding in urban areas, GE scenario  
304 shows to be better than BU scenario, but worse than GP scenario.

## 305 **5 Discussions**

### 306 **5.1 Source of uncertainties**

307 There are some limitations in our study, which is what we need to improve in the future. First, there is still more room to  
308 improve the accuracy of model prediction. In this study, the performance of the FLUS model is tested by kappa and OA  
309 measures, which shows a good range of prediction accuracy. In addition, this study proves that 16 driving factors contribute  
310 to the simulation and prediction of urban growth in Shanghai. The relationship between human and natural driving factors  
311 and land use change can be effectively integrated through the FLUS model embedded with an ANN, to obtain more realistic  
312 simulation results. However, if more influential drivers and the latest land cover are employed, the prediction would be  
313 having higher accuracy. Second, future flood risks in coastal areas are also not fully reflected through the use of  
314 hydrodynamic models, although it shows higher accuracy than the elevation area submergence method. On the one hand, this  
315 study is based on the modeling results of DEM data, which may overestimate or underestimate the simulation effect due to  
316 the error of DEM data. On the other hand, extreme storm surge and land subsidence data are combined to enhance the  
317 reliability of the extreme flood forecast in this study. However, the change of the impervious surface that affects hydrology  
318 is not yet considered in this study. When other land uses are converted to urban land uses, the risk of flooding will also  
319 greatly increase due to changes the of impervious surfaces. Therefore, it is necessary to dynamically adjust relevant factors  
320 affecting flood peak flows and risk in future forecasts to enhance the accuracy of prediction.

321 In the context of global climate change, extreme weather in the future may become more and more serious, so it is necessary  
322 to dynamically combine climate scenarios to develop more accurate flood risk delineation methods to guide urban planning  
323 in the future, and rely on new technology and equipment to provide data support. For example, unmanned aviation vehicles  
324 (UAVs) are deployed around the coastline to generate real-time information about weather conditions and sea-level changes  
325 (Cochrane et al., 2017). These tools will act as a complement to existing information and early warning systems, which also  
326 can provide guidance for coastal flood risk management and urban planning in the future. Overall, although uncertainty  
327 cannot be avoided when assessing coastal flood risk, the deviation of the proposed model output is within an acceptable  
328 range, which ensures the accuracy of coastal flood risk assessments.

## 329 **5.2 Recommendations on strategies and policies for urban adaptation to flooding**

330 In the twenty-first century, adapting to climate change and coastal flooding is a critical challenge for coastal cities. Human  
331 response to the impacts of flooding largely depends on the allocation of urban facilities and managers' planning for future  
332 urban development (Hunt and Watkiss, 2011). Shanghai is considered one of the most protected Chinese cities in terms of  
333 flood protection, yet it's the EAD/GDP (the Expected Annual Disruption, EAD), that is the direct damage to buildings and  
334 vehicles) ratio, which is as much as five times than in New York (Aerts et al., 2014). Therefore, there is an urgent need to  
335 adopt flood risk adaptation strategies in Shanghai.

336 We conducted a set of comparative experiments to analyze the coastal flood damage in Shanghai with and without flood  
337 walls (hard adaptation strategies). Our analysis considered the important effects of land subsidence and sea level rise on  
338 flood risk. We found that the current flood protection wall can reduce the flood losses due to climate change to a relatively  
339 low level (Supplementary Figure 2). In comparison, the flood protection wall constructed for the current conditions would  
340 reduce the flooded area under the RCP8.5 scenario by about 35 % and 36 % in 2030 and 2050, respectively. Furthermore,  
341 our results show that the area of future urban flood risk varies by scenario. Although the GE scenario performs higher than  
342 the GP scenario in terms of flood inundation area, this does not mean that the GE scenario is worse. From the cases of  
343 advanced flood risk management countries such as the Netherlands (Kabat et al., 2009; Song et al., 2018), an important  
344 success lesson for future flood protection design is to leave enough space along coasts for wetland migration and leave space  
345 for nature. In other words, "soft strategies" such as "working with rivers and nature" are considered in the flood protection  
346 measures. Therefore, from this perspective the GE scenario may be a more likely future development scenario among these  
347 three scenarios. Future, it is necessary to learn from the practical experience of advanced countries to strengthen the  
348 development and construction of coastal wetlands and tidal flat ecosystems, and further reduce the residual risk through the  
349 adaptive regulation of coastal ecosystems and other soft strategies. In addition, the implementation of "soft strategies" can  
350 increase the value of ecosystem services, increase biodiversity and carbon sequestration, and improve social welfare (Du et  
351 al., 2020).

## 352 **6 Conclusion**

353 Scenario-based assessment has been found to be a powerful approach in numerous flood risk studies. This study combines an  
354 urban growth model with a two-dimensional flood inundation model to not only simulate urban development dynamics more  
355 accurately, but also to discard the shortcomings of the traditional elevation inundation method of overestimating inundation  
356 areas. We have also tested the resilience of Shanghai to future different climate scenarios with the current flood wall. The  
357 results of the study are beneficial to local planners and coastal managers in making decisions of future protected areas and  
358 developments.

359 This study employed three urban development scenarios and detected the relationships of urbanization and climate changes  
360 in 2030 and 2050. The results of the study show that urban growth under the three scenario models manifests significant



361 differences in expansion trajectories, influenced by key factors such as infrastructure development and policy constraints.  
362 According to the predicted results of flood, new built-up areas are also potentially vulnerable areas of flood risk. New built-  
363 up areas under different scenarios show significant vulnerability and exposure risk under different climate scenarios, even  
364 with the support of flood bank and other hard structures. Additionally, the research provided significant insights into the  
365 range and spatial distribution of flood risk in future urban areas.

Deleted: potential

366 The current study is based on the multi-scenario analysis of RCP global warming scenarios. In the future, the shared  
367 socioeconomic pathways (SSPs) can be combined to predict land use change, which make urban development scenarios  
368 more realistic choices. The results of this study estimate the future urban flood exposure areas, but this does not mean that all  
369 flood-vulnerable areas will be flooded, only that in these areas, the probability of each possible occurrence is greater.  
370 Therefore, proper preparations (such as definition restricted development zones) can reduce the damage risk of future flood  
371 and build more resilient cities.

Deleted: multi

#### 372 **Author contributions**

373 Q. Sun and J. Fang designed the research; Q. Sun, K. Xu and X. Dang collected the data and carried out the experiments; Q.  
374 Sun wrote the draft; J. Fang, X. Dang, Y. Fang and M. Liu revised the manuscript; J. Fang, X. Li and M. Liu supervised and  
375 provided critical feedback. All authors contributed to the final version of the manuscript.

#### 376 **Competing interests**

377 The authors declare that they have no conflict of interest.

#### 378 **Funding source**

379 This work was supported by a grant from the National Natural Science Foundation of China (42001096, 41730646);  
380 Shanghai Sailing Program (19YF1413700); China Postdoctoral Science Foundation (2019M651429).; East China Normal  
381 University Institute of Belt and Road & Global Development (ECNU-BRGD-202106), and the National Key R&D Program  
382 of China (2017YFE0100700).

#### 383 **References**

384 Aerts, J. C. J. H., Botzen, W. J. W., Emanuel, K., Lin, N., De Moel, H. and Michel-Kerjan, E. O.: Climate adaptation:  
385 Evaluating flood resilience strategies for coastal megacities, *Science* (80-. ), 344(6183), 473–475,  
386 doi:10.1126/science.1248222, 2014.

389 Bates, P. D., Horritt, M. S. and Fewtrell, T. J.: A simple inertial formulation of the shallow water equations for efficient two-  
390 dimensional flood inundation modelling, *J. Hydrol.*, 387(1–2), 33–45, doi:10.1016/j.jhydrol.2010.03.027, 2010.

391 Berke, P. R., Malecha, M. L., Yu, S., Lee, J. and Masterson, J. H.: Plan integration for resilience scorecard: evaluating  
392 networks of plans in six US coastal cities, *J. Environ. Plan. Manag.*, 62(5), 901–920,  
393 doi:10.1080/09640568.2018.1453354, 2019.

394 Bouwer, L. M.: Next-generation coastal risk models, *Nat. Clim. Chang.*, 8(9), 765–766, doi:10.1038/s41558-018-0262-2,  
395 2018.

396 Chen, G., Li, X., Liu, X., Chen, Y., Liang, X., Leng, J., Xu, X., Liao, W., Qiu, Y., Wu, Q. and Huang, K.: Global projections  
397 of future urban land expansion under shared socioeconomic pathways, *Nat. Commun.*, 11(1), 537, doi:10.1038/s41467-  
398 020-14386-x, 2020.

399 Cochrane, L., Cundill, G., Ludi, E., New, M., Nicholls, R. J., Wester, P., Cantin, B., Murali, K. S., Leone, M., Kituyi, E. and  
400 Landry, M. E.: A reflection on collaborative adaptation research in Africa and Asia, *Reg. Environ. Chang.*, 17(5), 1553–  
401 1561, doi:10.1007/s10113-017-1140-6, 2017.

402 Van Coppenolle, R. and Temmerman, S.: A global exploration of tidal wetland creation for nature-based flood risk  
403 mitigation in coastal cities, *Estuar. Coast. Shelf Sci.*, 226, 106262, doi:10.1016/j.ecss.2019.106262, 2019.

404 Du, S., Van Rompaey, A., Shi, P. and Wang, J.: A dual effect of urban expansion on flood risk in the Pearl River Delta  
405 (China) revealed by land-use scenarios and direct runoff simulation, *Nat. Hazards*, 77(1), 111–128,  
406 doi:10.1007/s11069-014-1583-8, 2015.

407 Du, S., Scussolini, P., Ward, P. J., Zhang, M., Wen, J., Wang, L., Koks, E., Diaz-Loaiza, A., Gao, J., Ke, Q. and Aerts, J. C.  
408 J. H.: Hard or soft flood adaptation? Advantages of a hybrid strategy for Shanghai, *Glob. Environ. Chang.*, 61, 102037,  
409 doi:https://doi.org/10.1016/j.gloenvcha.2020.102037, 2020.

410 Dullo, T. T., Darkwah, G. K., Gangrade, S., Morales-Hernández, M., Sharif, M. B., Kalyanapu, A. J., Kao, S. C., Ghafoor, S.  
411 and Ashfaq, M.: Assessing climate-change-induced flood risk in the Conasauga River watershed: An application of  
412 ensemble hydrodynamic inundation modeling, *Nat. Hazards Earth Syst. Sci.*, 21(6), 1739–1757, doi:10.5194/nhess-21-  
413 1739-2021, 2021.

414 Fang, J., Lincke, D., Brown, S., Nicholls, R. J., Wolff, C., Merken, J. L., Hinkel, J., Vafeidis, A. T., Shi, P. and Liu, M.:  
415 Coastal flood risks in China through the 21st century – An application of DIVA, *Sci. Total Environ.*, 704, 135311,  
416 doi:10.1016/j.scitotenv.2019.135311, 2020.

417 Fang, J., Wahl, T., Zhang, Q., Muis, S., Hu, P., Fang, J., Du, S., Dou, T. and Shi, P.: Extreme sea levels along coastal China:  
418 uncertainties and implications, *Stoch. Environ. Res. Risk Assess.*, 35(2), 405–418, doi:10.1007/s00477-020-01964-0,  
419 2021.

420 Gori, A., Blessing, R., Juan, A., Brody, S. and Bedient, P.: Characterizing urbanization impacts on floodplain through  
421 integrated land use, hydrologic, and hydraulic modeling, *J. Hydrol.*, 568, 82–95, doi:10.1016/j.jhydrol.2018.10.053,  
422 2019.

423 Gounaridis, D., Choriantopoulos, I., Symeonakis, E. and Koukoulas, S.: A Random Forest-Cellular Automata modelling  
424 approach to explore future land use/cover change in Attica (Greece), under different socio-economic realities and  
425 scales, *Sci. Total Environ.*, 646, 320–335, doi:10.1016/j.scitotenv.2018.07.302, 2019.

426 Hallegatte, S., Green, C., Nicholls, R. J. and Corfee-Morlot, J.: Future flood losses in major coastal cities, *Nat. Clim. Chang.*,  
427 3(9), 802–806, doi:10.1038/nclimate1979, 2013.

428 Haynes, P., Hehl-Lange, S. and Lange, E.: Mobile Augmented Reality for Flood Visualisation, *Environ. Model. Softw.*, 109,  
429 380–389, doi:10.1016/j.envsoft.2018.05.012, 2018.

430 He, C., Liu, Z., Wu, J., Pan, X., Fang, Z., Li, J. and Bryan, B. A.: Future global urban water scarcity and potential solutions,  
431 *Nat. Commun.*, 12(1), 1–11, doi:10.1038/s41467-021-25026-3, 2021.

432 Hoch, J. M., Eilander, D., Ikeuchi, H., Baart, F. and Winsemius, H. C.: Evaluating the impact of model complexity on flood  
433 wave propagation and inundation extent with a hydrologic-hydrodynamic model coupling framework, *Nat. Hazards*  
434 *Earth Syst. Sci.*, 19(8), 1723–1735, doi:10.5194/nhess-19-1723-2019, 2019.

435 Hunt, A. and Watkiss, P.: Climate change impacts and adaptation in cities: A review of the literature, *Clim. Change*, 104(1),  
436 13–49, doi:10.1007/s10584-010-9975-6, 2011.

437 Huong, H. T. L. and Pathirana, A.: Urbanization and climate change impacts on future urban flooding in Can Tho city,  
438 Vietnam, *Hydrol. Earth Syst. Sci.*, 17(1), 379–394, doi:10.5194/hess-17-379-2013, 2013.

439 IPCC: Climate Change 2014: Impacts, Adaptation, and Vulnerability. Part A: Global and Sectoral Aspects. Contribution of  
440 Working Group II to the Fifth Assessment Report of the Intergovernmental Panel on Climate Change, Cambridge  
441 University Press, Cambridge, UK., 2014.

442 Kabat, P., Fresco, L. O., Stive, M. J. F., Veerman, C. P., van Alphen, J. S. L. J., Parmet, B. W. A. H., Hazeleger, W. and  
443 Katsman, C. A.: Dutch coasts in transition, *Nat. Geosci.*, 2(7), 450–452, doi:10.1038/ngeo572, 2009.

444 Kim, Y. and Newman, G.: Advancing scenario planning through integrating urban growth prediction with future flood risk  
445 models, *Comput. Environ. Urban Syst.*, 82, 101498, doi:https://doi.org/10.1016/j.compenvurbsys.2020.101498, 2020.

446 Kopp, R. E., DeConto, R. M., Bader, D. A., Hay, C. C., Horton, R. M., Kulp, S., Oppenheimer, M., Pollard, D. and Strauss,  
447 B. H.: Evolving understanding of Antarctic ice-sheet physics and ambiguity in probabilistic sea-level projections, *arXiv*,  
448 2017.

449 Lai, C., Shao, Q., Chen, X., Wang, Z., Zhou, X., Yang, B. and Zhang, L.: Flood risk zoning using a rule mining based on ant  
450 colony algorithm, *J. Hydrol.*, 542, 268–280, doi:https://doi.org/10.1016/j.jhydrol.2016.09.003, 2016.

451 Liang, X., Liu, X., Li, X., Chen, Y., Tian, H. and Yao, Y.: Delineating multi-scenario urban growth boundaries with a CA-  
452 based FLUS model and morphological method, *Landsc. Urban Plan.*, 177, 47–63,  
453 doi:10.1016/j.landurbplan.2018.04.016, 2018.

454 Lin, W., Sun, Y., Nijhuis, S. and Wang, Z.: Scenario-based flood risk assessment for urbanizing deltas using future land-use  
455 simulation (FLUS): Guangzhou Metropolitan Area as a case study, *Sci. Total Environ.*, 739, 139899,  
456 doi:10.1016/j.scitotenv.2020.139899, 2020.

457 Liu, J., Kuang, W., Zhang, Z., Xu, X., Qin, Y., Ning, J., Zhou, W., Zhang, S., Li, R., Yan, C., Wu, S., Shi, X., Jiang, N., Yu,  
458 D., Pan, X. and Chi, W.: Spatiotemporal characteristics, patterns and causes of land use changes in China since the late  
459 1980s, *Dili Xuebao/Acta Geogr. Sin.*, 69(1), 3–14, doi:10.11821/dlxb201401001, 2014.

460 Liu, X., Liang, X., Li, X., Xu, X., Ou, J., Chen, Y., Li, S., Wang, S. and Pei, F.: A future land use simulation model (FLUS)  
461 for simulating multiple land use scenarios by coupling human and natural effects, *Landsc. Urban Plan.*, 168, 94–116,  
462 doi:10.1016/j.landurbplan.2017.09.019, 2017.

463 Muis, S., Güneralp, B., Jongman, B., Aerts, J. C. J. H. and Ward, P. J.: Flood risk and adaptation strategies under climate  
464 change and urban expansion: A probabilistic analysis using global data, *Sci. Total Environ.*, 538, 445–457,  
465 doi:10.1016/j.scitotenv.2015.08.068, 2015.

466 Muis, S., Verlaan, M., Winsemius, H. C., Aerts, J. C. J. H. and Ward, P. J.: A global reanalysis of storm surges and extreme  
467 sea levels, *Nat. Commun.*, 7, 11969, doi:10.1038/ncomms11969, 2016.

468 Nithila Devi, N., Sridharan, B. and Kuiry, S. N.: Impact of urban sprawl on future flooding in Chennai city, India, *J. Hydrol.*,  
469 574, 486–496, doi:10.1016/j.jhydrol.2019.04.041, 2019.

470 O’Loughlin, F. E., Neal, J., Schumann, G. J. P., Beighley, E. and Bates, P. D.: A LISFLOOD-FP hydraulic model of the  
471 middle reach of the Congo, *J. Hydrol.*, 580, doi:10.1016/j.jhydrol.2019.124203, 2020.

472 Parodi, M. U., Giardino, A., Van Dongeren, A., Pearson, S. G., Bricker, J. D. and Reniers, A. J. H. M.: Uncertainties in  
473 coastal flood risk assessments in small island developing states, *Nat. Hazards Earth Syst. Sci.*, 20(9), 2397–2414,  
474 doi:10.5194/nhess-20-2397-2020, 2020.

475 Parris, A., Bromirski, P., Burkett, V., Cayan, D., Culver, M., Hall, J., Horton, R., Knuuti, K., Moss, R., Obeysekera, J.,  
476 Sallenger, A. and Weiss, J.: Global Sea Level Rise Scenarios for the US National Climate Assessment, NOAA Tech  
477 Memo OAR CPO, 1–37, doi:https://scenarios.globalchange.gov/sites/default/files/NOAA\_SLR\_r3\_0.pdf, 2012.

478 Pecl, G. T., Araújo, M. B., Bell, J. D., Blanchard, J., Bonebrake, T. C., Chen, I. C., Clark, T. D., Colwell, R. K., Danielsen,  
479 F., Evengård, B., Falconi, L., Ferrier, S., Frusher, S., Garcia, R. A., Griffis, R. B., Hobday, A. J., Janion-Scheepers, C.,  
480 Jarzyna, M. A., Jennings, S., Lenoir, J., Linnertved, H. I., Martin, V. Y., McCormack, P. C., McDonald, J., Mitchell, N.  
481 J., Mustonen, T., Pandolfi, J. M., Pettorelli, N., Popova, E., Robinson, S. A., Scheffers, B. R., Shaw, J. D., Sorte, C. J.  
482 B., Strugnell, J. M., Sunday, J. M., Tuanmu, M. N., Vergés, A., Villanueva, C., Wernberg, T., Wapstra, E. and  
483 Williams, S. E.: Biodiversity redistribution under climate change: Impacts on ecosystems and human well-being,  
484 *Science (80-. )*, 355(6332), doi:10.1126/science.aai9214, 2017.

485 Rajib, A., Liu, Z., Merwade, V., Tavakoly, A. A. and Follum, M. L.: Towards a large-scale locally relevant flood inundation  
486 modeling framework using SWAT and LISFLOOD-FP, *J. Hydrol.*, 581, 124406, doi:10.1016/j.jhydrol.2019.124406,  
487 2020.

488 Ramaswami, A., Russell, A. G., Culligan, P. J., Rahul Sharma, K. and Kumar, E.: Meta-principles for developing smart,  
489 sustainable, and healthy cities, *Science (80-. )*, 352, 940–943, doi:10.1126/science.aaf7160, 2016.

490 Reckien, D., Salvia, M., Heidrich, O., Church, J. M., Pietrapertosa, F., De Gregorio-Hurtado, S., D'Alonzo, V., Foley, A.,  
491 Simoes, S. G., Krkoška Lorencová, E., Orru, H., Orru, K., Wejs, A., Flacke, J., Olazabal, M., Geneletti, D., Feliu, E.,  
492 Vasilie, S., Nador, C., Krook-Riekkola, A., Matosović, M., Fokaides, P. A., Ioannou, B. I., Flamos, A., Spyridaki, N.  
493 A., Balzan, M. V., Fülöp, O., Paspaldzhiev, I., Grafakos, S. and Dawson, R.: How are cities planning to respond to  
494 climate change? Assessment of local climate plans from 885 cities in the EU-28, *J. Clean. Prod.*, 191, 207–219,  
495 doi:10.1016/j.jclepro.2018.03.220, 2018.

496 Shan, X., Yin, J. and Wang, J.: Risk assessment of shanghai extreme flooding under the land use change scenario, *Nat.*  
497 *Hazards*, 110(2), 1039–1060, doi:10.1007/s11069-021-04978-1, 2022.

498 Song, J., Fu, X., Wang, R., Peng, Z.-R. and Gu, Z.: Does planned retreat matter? Investigating land use change under the  
499 impacts of flooding induced by sea level rise, *Mitig. Adapt. Strateg. Glob. Chang.*, 23(5), 703–733,  
500 doi:10.1007/s11027-017-9756-x, 2018.

501 Sosa, J., Sampson, C., Smith, A., Neal, J. and Bates, P.: A toolbox to quickly prepare flood inundation models for  
502 LISFLOOD-FP simulations, *Environ. Model. Softw.*, 123, 104561, doi:https://doi.org/10.1016/j.envsoft.2019.104561,  
503 2020.

504 Sun, L., Chen, J., Li, Q. and Huang, D.: Dramatic uneven urbanization of large cities throughout the world in recent decades,  
505 *Nat. Commun.*, 11(1), 5366, doi:10.1038/s41467-020-19158-1, 2020.

506 Tessler, Z. D., Vorosmarty, C. J., Grossberg, M., Gladkova, I., Aizenman, H., Syvitski, J. P. M. and Foufoula-Georgiou, E.:  
507 Profiling risk and sustainability in coastal deltas of the world, *Science* (80-. ), 349, 638–643,  
508 doi:10.1126/science.aab3574, 2015.

509 United Nations: Factsheet: People and oceans., 2017.

510 United Nations: 2018 Revision of World Urbanization Prospects. [online] Available from: <https://population.un.org/wup/>,  
511 2018.

512 Vousdoukas, M. I., Mentaschi, L., Voukouvalas, E., Verlaan, M., Jevrejeva, S., Jackson, L. P. and Feyen, L.: Global  
513 probabilistic projections of extreme sea levels show intensification of coastal flood hazard, *Nat. Commun.*, 9(1), 1–12,  
514 doi:10.1038/s41467-018-04692-w, 2018.

515 Wang, Z., Lai, C., Chen, X., Yang, B., Zhao, S. and Bai, X.: Flood hazard risk assessment model based on random forest, *J.*  
516 *Hydrol.*, 527, 1130–1141, doi:10.1016/j.jhydrol.2015.06.008, 2015.

517 Wen, K.: *Meteorological Disasters in China* (in Chinese), China Meteorological Press, Beijing, China., 2006.

518 Wing, O. E. J., Sampson, C. C., Bates, P. D., Quinn, N., Smith, A. M. and Neal, J. C.: A flood inundation forecast of  
519 Hurricane Harvey using a continental-scale 2D hydrodynamic model, *J. Hydrol. X*, 4, 100039,  
520 doi:https://doi.org/10.1016/j.hydroa.2019.100039, 2019.

521 Xian, S., Yin, J., Lin, N. and Oppenheimer, M.: Influence of risk factors and past events on flood resilience in coastal  
522 megacities: Comparative analysis of NYC and Shanghai, *Sci. Total Environ.*, 610–611, 1251–1261,  
523 doi:10.1016/j.scitotenv.2017.07.229, 2018.

524 Xu, K., Fang, J., Fang, Y., Sun, Q., Wu, C. and Liu, M.: The Importance of Digital Elevation Model Selection in Flood  
525 Simulation and a Proposed Method to Reduce DEM Errors: A Case Study in Shanghai, *Int. J. Disaster Risk Sci.*,  
526 doi:10.1007/s13753-021-00377-z, 2021.

527 Xu, W. (Ato) and Yang, L.: Evaluating the urban land use plan with transit accessibility, *Sustain. Cities Soc.*, 45, 474–485,  
528 doi:10.1016/j.scs.2018.11.042, 2019.

529 Xu, X., Liu, J., Zhang, Z., Zhou, W., Zhang, S., Li, R., Yan, C., Wu, S. and Shi, X.: A Time Series Land Ecosystem  
530 Classification Dataset of China in Five-Year Increments (1990–2010), *J. Glob. Chang. Data Discov.*, 1(1), 52–59,  
531 doi:10.3974/geodp.2017.01.08, 2017.

532 Yin, J., Yu, D., Yin, Z., Wang, J. and Xu, S.: Modelling the combined impacts of sea-level rise and land subsidence on storm  
533 tides induced flooding of the Huangpu River in Shanghai, China, *Clim. Change*, 119(3–4), 919–932,  
534 doi:10.1007/s10584-013-0749-9, 2013.

535 Yin, J., Jonkman, S., Lin, N., Yu, D., Aerts, J., Wilby, R., Pan, M., Wood, E., Bricker, J., Ke, Q., Zeng, Z., Zhao, Q., Ge, J.  
536 and Wang, J.: Flood Risks in Sinking Delta Cities: Time for a Reevaluation?, *Earth's Futur.*, 8(8),  
537 doi:10.1029/2020EF001614, 2020.

538 Zhai, Y., Yao, Y., Guan, Q., Liang, X., Li, X., Pan, Y., Yue, H., Yuan, Z. and Zhou, J.: Simulating urban land use change by  
539 integrating a convolutional neural network with vector-based cellular automata, *Int. J. Geogr. Inf. Sci.*, 34(7), 1475–  
540 1499, doi:10.1080/13658816.2020.1711915, 2020.

541 Zhao, G., Bates, P. and Neal, J.: The Impact of Dams on Design Floods in the Conterminous US, *Water Resour. Res.*, 56(3),  
542 1–15, doi:10.1029/2019WR025380, 2020.

543 Zhao, L., Song, J. and Peng, Z.-R.: Modeling Land-Use Change and Population Relocation Dynamics in Response to  
544 Different Sea Level Rise Scenarios: Case Study in Bay County, Florida, *J. Urban Plan. Dev.*, 143(3), 04017012,  
545 doi:10.1061/(asce)up.1943-5444.0000398, 2017.

546 Zhou, L., Dang, X., Sun, Q. and Wang, S.: Multi-scenario simulation of urban land change in Shanghai by random forest and  
547 CA-Markov model, *Sustain. Cities Soc.*, 55, 102045, doi:10.1016/j.scs.2020.102045, 2020.

548 Zhou, Q., Leng, G., Su, J. and Ren, Y.: Comparison of urbanization and climate change impacts on urban flood volumes:  
549 Importance of urban planning and drainage adaptation, *Sci. Total Environ.*, 658, 24–33,  
550 doi:https://doi.org/10.1016/j.scitotenv.2018.12.184, 2019.

551 Xu, X.: China GDP Spatial Distribution Kilometer Grid Dataset [dataset], <http://www.resdc.cn/DOI/doi.aspx?DOIid=33>,  
552 2017a.

553 Xu, X.: China Population Spatial Distribution Kilometer Grid Dataset [dataset],  
554 <http://www.resdc.cn/DOI/DOI.aspx?DOIid=32>, 2017b.